NANO · MICRO small
www.small-journal.com

Influence of Lithium Diffusion into Copper Current Collectors on Lithium Electrodeposition in Anode-Free Lithium-Metal Batteries

*Yu-Kai Huang, Heyin Chen, and Leif Nyholm**

The development of "anode-free" lithium-metal batteries with high energy densities is, at present, mainly limited by the poor control of the nucleation of lithium directly on the copper current collector, especially in conventional carbonate electrolytes. It is therefore essential to improve the understanding of the lithium nucleation process and its interactions with the copper substrate. In this study, it is shown that diffusion of lithium into the copper substrate, most likely via the grain boundaries, can significantly influence the nucleation process. Such diffusion makes it more difficult to obtain a great number of homogeneously distributed lithium nuclei on the copper surface and thus leads to inhomogeneous electrodeposition. It is, however, demonstrated that the nucleation of lithium on copper is significantly improved if an initial chemical prelithiation of the copper surface is performed. This prelithiation saturates the copper surface with lithium and hence decreases the influence of lithium diffusion via the grain boundaries. In this way, the lithium nucleation can be made to take place more homogenously, especially when a short potentiostatic nucleation pulse that can generate a large number of nuclei on the surface of the copper substrate is applied.

1. Introduction

With increasing demands for lithium-based batteries that have higher energy densities, access to better negative electrode materials becomes crucial. Lithium metal which has a very high theoretic capacity (i.e., 3860 mAh g^{-1}) and a very low standard potential (i.e., −3.04 V vs standard hydrogen electrode) can be considered the ideal negative electrode material for next-generation lithium-based batteries. In order to fully exploit the merits of lithium-metal electrodes in lithium-based batteries so that the gravimetric energy density (Wh kg^{-1}) and the volumetric energy density (Wh L^{-1}) can be increased, a configuration with close-to-zero lithium-metal excess should be adopted. However, from a practical point of view, it is very difficult to use a very thin (<10 μm) lithium-metal foil directly as the lithium-metal electrode without any current collector. Therefore, one way to do this would be to electrodeposit (and then strip) the lithium directly on (from) the negative electrode current collector (i.e., battery-grade copper foil) in the absence of any extra "pre-plated" lithium metal.[1–3] The "anode-material-free" (or "anode-free") lithium-metal batteries can not only offer high energy densities but also have production advantages. Since there is no need to handle thin lithium-metal foils, the manufacturing of anode-free batteries would be more compatible with contemporary assembly lines. However, to be able to consistently use anode-free lithium batteries, the problems associated with the formation of dead lithium, porous lithium, and lithium dendrites during lithium electrodeposition on copper current collectors must be solved.[2]

Although the electrodeposition of lithium on a copper current collector differs from that on a lithium-metal electrode, the above-mentioned problems are essentially the same in both cases. The problems stem from an inability to properly control the lithium nucleation process so that 2D homogeneous lithium electrodeposition can be obtained. Many strategies have been proposed to improve the lithium electrodeposition in anode-free cells.[2,4–6] Among them, the development of new electrolyte formulations, affecting the Li^+ solvation structure and/or the compositions and morphologies of the solid electrolyte interphase (SEI) layer, constitutes the major chemistry-related approach.[3,7–15] Other material-related approaches involve i) modifications of the copper current collectors by synthesizing 3D structures to lower the local current densities and encapsulate the electrodeposited lithium, ii) designs of artificial SEI layers that are more stable during the lithium electrodeposition, and/or iii) coating so-called "lithiophilic" materials on the copper surface to facilitate the nucleation of lithium.[16–27]

So far, fundamental electrochemical approaches do not appear to have been used to control the nucleation and growth of lithium on copper substrates. This is surprising since electrodeposition

Y.-K. Huang, H. Chen, L. Nyholm
Department of Chemistry – Ångström Laboratory
Uppsala University
Box 538, Uppsala SE-751 21, Sweden
E-mail: leif.nyholm@kemi.uu.se

The ORCID identification number(s) for the author(s) of this article can be found under https://doi.org/10.1002/smll.202306829

DOI: 10.1002/smll.202306829

theory and practice have been maturely developed and widely used for metal electrodeposition in other fields.[28,29] According to the classical electrodeposition theory, the critical free energy for the nucleation, ΔG_c, and the critical radius of the nuclei, r_c, can be calculated as

$$\Delta G_c = \frac{16\pi M^2 \gamma^3}{3\rho^2 n^2 F^2 \eta^2} \quad (1)$$

$$r_c = \frac{-2M\gamma}{nF\rho\eta} \quad (2)$$

where M is the molecular weight, γ is the molar surface free energy, ρ is the density of the electrodeposit, n is the number of electrons involved in the electrodeposition reaction, F is the Faraday constant, and η is the overpotential.[28] The critical free energy represents the energy barrier that needs to be overcome for the nucleation to take place and hence affects the nucleation rate, whereas the critical radius defines the minimum size of the nuclei needed for the nuclei to "survive" and then grow. Sufficiently small nuclei are hence not stable and tend to undergo "dissolution." For the electrodeposition of a certain metal, the major variables are the surface free energy, γ, and the overpotential, η.

The surface free energy may vary with temperature and thus change the critical free energy for the nucleation as well as the nucleation rate.[30] Besides, it also influences the electrodeposition morphologies of lithium as observed in previous studies in which the temperature was increased to 40 or 60 °C.[31–34]

According to the abovementioned equations, the use of a larger η will lead to a decrease in both ΔG_c and r_c. Hence, the nucleation process should then be facilitated given that more clusters can reach the critical radius needed to form stable nuclei with a lower energy barrier. A larger η will therefore lead to the formation of a greater number of small(er) nuclei on the electrode surface, whereas a small η will lead to the formation of a few large(r) nuclei preferentially at the most favorable sites on the substrate. This effect has been observed mainly by studying the influences of variations in the applied current on the obtained lithium electrodeposits, and the nuclei density was empirically found to be proportional to the cubic power of the overpotential in an ether-based electrolyte.[35–39]

However, there does not appear to be any explicit studies describing the use of an applied overpotential to electrochemically control the nucleation of lithium in conjunction with the anode-free concept. In a lithium symmetric cell configuration (i.e., lithium electrodeposition on a lithium-metal electrode), Rehnlund et al., however, demonstrated that a large number of homogeneously-distributed lithium nuclei could be obtained by applying a 10 ms long reductive potentiostatic pulse during the initial nucleation stage after decreasing the concentration of the $LiPF_6$ electrolyte from 1.0 to 0.02 M.[40] By decreasing the $LiPF_6$ concentration, it became possible to reach a sufficiently large overpotential during the nucleation pulse to form nuclei all over the electrode surface. Homogeneous 2D lithium electrodeposition could then be attained by allowing these nuclei to grow using either conventional constant-current (CC) or pulsed-current deposition. The question is then if this approach likewise is applicable when electrodepositing lithium on copper substrates.

At this point it should be recalled that there are several reasons why electrodeposition of lithium on a copper substrate would be different from that of lithium on a lithium-metal electrode.[41] Due to the presence of a native oxide/hydroxide layer on the copper surface, conversion reactions yielding a surface layer composed of Cu nanoparticles and Li_2O will occur on the very first reduction step. This and the formation of a SEI layer due to the reduction of the electrolyte at lower potentials hence take place prior to the onset of lithium electrodeposition on copper.[42–47] Moreover, the potential for the onset of lithium electrodeposition on copper should depend on the activity of elemental lithium at the copper surface as can be predicted by the Nernst equation. As the latter activity should be much lower than unity, the electrodeposition of lithium should hence thermodynamically start at a potential more positive than 0 V versus Li^+/Li in a 1.0 M $LiPF_6$ electrolyte. As the activity of lithium in the surface region of the copper increases, the electrodeposition potential should gradually be shifted toward lower potentials and eventually 0 V versus Li^+/Li in a 1.0 M $LiPF_6$ electrolyte. The latter should happen once the copper surface has been coated with a layer of lithium. At that point, the lithium covered copper substrate would thus behave like a lithium-metal electrode. Such a lithium activity effect should clearly not be present when electrodepositing lithium on a lithium-metal electrode. In addition, it has been shown that the electrodeposition of lithium on copper results in lithium diffusing into the copper.[44,48–52] This is in fact expected (although copper does not form an alloy with lithium) as a solid solution with up to 13–14 at% Li can form according to the Cu-Li phase diagram.[53] Furthermore, the fact that lithium can enter and move through copper has actually been exploited to develop protective copper coatings on silicon nanomaterials for lithium-ion batteries.[54,55] The absence of the formation of an alloy between lithium and copper is, nevertheless, still often used to motivate the choice of copper as the material for negative electrode current collectors in lithium-ion batteries.

Using inductively coupled plasma-atomic emission spectroscopy (ICP-AES), Rehnlund et al. found significant amounts of lithium in copper, nickel, and titanium foils after they had been in contact with elemental lithium for one week at 50 °C.[48] In another study by Rehnlund et al., a layer of lithium with a thickness of about 25 nm was electrodeposited on copper nanorods in an attempt to manufacture a 3D lithium nanoelectrode.[44] The electrodeposited lithium was, however, found to diffuse into the nanorods, resulting in a rapid capacity loss of the lithium nanorod electrode. These results clearly show that lithium can diffuse into copper and that the effect of this diffusion can be readily seen after electrodepositing a small amount of lithium (as would be the case during the lithium nucleation stage). Using operando neutron diffraction to track the spatial distribution of lithium during lithium electrodeposition and stripping on copper, Lv et al. found that some lithium was actually taken up by the copper substrates during the electrodeposition step.[49] Moreover, the authors observed that the amount of lithium in the copper increased when the electrodeposition current was increased. The abovementioned findings thus further indicate that diffusion of lithium into copper, most likely via the grain boundaries, will take place simultaneously while lithium is being electrodeposited on copper. This raises the following scientific questions: How does the diffusion of lithium into the copper substrate affect

the lithium nucleation and hence the possibilities of attaining 2D electrodeposition of lithium on copper?

In this work, the abovementioned questions are addressed based on a series of lithium electrodeposition experiments on copper substrates using three-electrode cells. The purpose of the experiments is to study the possibilities of using a potentiostatic nucleation pulse to improve the nucleation of lithium and hence the possibilities to attain 2D nucleation and growth of lithium on copper. In this process the influence of the lithium diffusion into the copper substrates on the formation of stable lithium nuclei clearly needs to be considered. It is demonstrated that the diffusion of lithium into copper affects the initial nucleation process significantly. As this effect decreases the density of lithium nuclei on the copper surface, more inhomogeneous electrodeposits are obtained. The nucleation of lithium on copper substrates is hence shown to be more complicated than that on lithium-metal electrodes. It is further demonstrated that the influence of the lithium diffusion can be decreased by chemically prelithiating the surfaces of the copper substrates. This prelithiation hinders the lithium diffusion during the nucleation stage, and hence allows the formation of a larger number of homogeneously distributed lithium nuclei, especially during the application of a potentiostatic nucleation pulse, which results in more homogeneous and more compact lithium electrodeposits.

2. Results and Discussion

As mentioned above, the main aims of this work are to evaluate if the application of a potentiostatic nucleation pulse can be used to obtain 2D nucleation (and then growth) of lithium on copper, and to investigate how the nucleation is affected by the diffusion of lithium into the copper. To address these issues, electrodeposition experiments were performed with three-electrode cells containing two lithium metal electrodes as the counter and reference electrodes, a copper substrate as the working electrode and LP40 (i.e., 1.0 M $LiPF_6$ in ethylene carbonate (EC):diethyl carbonate (DEC) = 1:1 (v/v)) based electrolytes. The three-electrode setup allowed the application of a reductive potentiostatic nucleation pulse to the copper working electrode and thus the evaluation of the use of such a pulse as a means of controlling the density of the nuclei generated on the copper surface. To obtain homogeneously 2D lithium electrodeposition it should clearly be advantageous to generate nuclei of about the same size everywhere on the surface of the electrode.[40] As the formed nuclei then should be allowed to grow under, e.g., conventional CC conditions, it is important that the nucleation is instantaneous and that the formed nuclei are stable on the electrode surface. Given that lithium can diffuse into copper, the nucleation can be expected to be a larger problem when nanometer-sized lithium nuclei are formed on copper substrates than on lithium-metal electrodes. Conventional LP40 electrolyte as well as a diluted version of this electrolyte was employed in this study as the electrodeposition of lithium is known to perform poorly in such EC-based electrolytes containing no additive. This should facilitate the study of the lithium nucleation (and then growth) as the detection of changes in the process(es) should be easier. Besides, electrolytes containing $LiPF_6$ dissolved in EC-based solvent mixtures are still the dominant electrolytes in conjunction with the lithium-based batteries. An improved understanding of the lithium nucleation on copper substrates in this type of electrolytes should clearly also facilitate the development of anode-free cells. Since it is known that the electrochemical performance of the cell is relatively insensitive to different morphologies of the electrodeposited lithium, the questions raised above will mainly be discussed based on comparisons of the obtained lithium morphologies using scanning electron microscopy (SEM).[40,56]

As illustrated in **Figure 1**, three different electrochemical protocols were used in the electrodeposition experiments of this study. Here, it should also be noted that the as-assembled cells were kept under open-circuit condition for 30 min prior to the electrodeposition experiments. In all the protocols, a CC step including a low current density (i.e., −0.1 mA cm^{-2}) was first used to bring the cell voltage down to 0 V to "precondition" the copper substrate (i.e., to reduce the copper oxide(s)/hydroxide(s)) present at the surface, and to form an SEI layer).[42–47] Electrodeposition of lithium was subsequently performed employing CC deposition, pulsed-current deposition, or pulsed-current deposition in the presence of a preceding potentiostatic nucleation pulse, as shown in Figure 1a–c, respectively. In contrast to conventional CC deposition, pulsed-current deposition is based on periodically-repeated application of galvanostatic pulses separated by open-circuit periods. The major purpose of the open-circuit periods is to provide time for the diffusion layers to be replenished, which is particularly important when electrodepositing on a rough or porous electrode surface.[57] The t_{on} should be longer than the time required to fully charge the electrical double layer (which depends on the current used, the double-layer capacitance of the (electrodeposited) substrate and the electrolyte resistance), but short enough not to give rise to the mass transport issues typically seen during conventional CC deposition.[57–59] Moreover, the t_{off} and the duty cycle, defined as the ratio of t_{on} to $t_{on} + t_{off}$, should be optimized to obtain a well-defined electrodeposit within reasonable time. In this study, the pulsed-current deposition was performed with t_{on}:t_{off} = 1 ms:3 ms or 5 ms:25 ms. Last but not least, a relatively low electrodeposition capacity (i.e., 0.5 mAh cm^{-2}) was chosen since this facilitates studies of the nucleation as well as the influence of the copper substrates, by studying the morphologies of the obtained lithium electrodeposits with SEM, without complicating the experiments too much.[37,60]

The morphologies of the electrodeposited lithium obtained on the pure copper substrates using the different electrodeposition protocols and electrolytes (see the Experimental Section) are shown in **Figure 2**. As can be seen in Figure 2a,b, inhomogeneous electrodeposits were obtained for conventional CC deposition in the LP40 electrolyte with the formation of inhomogeneously distributed lithium "islands" of different sizes and "networks" of undesirable lithium "threads" on the substrate surface.[19,27] This may stem from the fact that the lithium nuclei were preferentially formed at the most electrochemically favorable sites on the copper surface, in agreement with previous findings for Li|Li symmetric cells.[40,56] The fact that analogous results were seen for copper substrates and lithium-metal electrodes indicates that inhomogeneous lithium nucleation is a general problem that needs to be solved in order to attain 2D lithium nucleation (and then growth).

According to the nucleation theory, providing a large overpotential, e.g., via the use of a potentiostatic nucleation pulse with a sufficiently large pulse height, should result in a dramatic

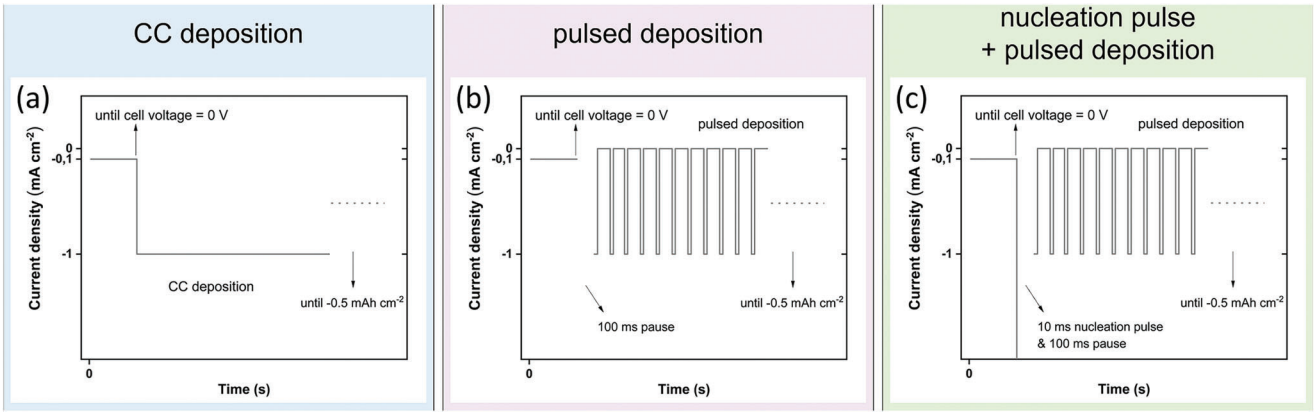

Figure 1. The protocols used in the lithium electrodeposition experiments, featuring a) conventional CC deposition, b) pulsed-current deposition, and c) a potentiostatic nucleation pulse followed by pulsed-current deposition. The pulsed-current deposition was carried out either with t_{on}:t_{off} = 1 ms:3 ms or 5 ms:25 ms. The different background colors, representing the corresponding protocols, are also used in the relevant figures below.

increase in the density of lithium nuclei on the electrode surface. This may enable instantaneous homogenous nucleation of a multitude of similarly sized lithium nuclei all over the copper surface which should then facilitate the attainment of 2D (rather than the typically obtained 3D) lithium growth. Experiments, in which a potentiostatic nucleation pulse was applied at the very beginning of the electrodeposition step, were therefore performed. Figure 2c,d show the lithium electrodeposits obtained with a potentiostatic pulse of −0.8 V which was applied after the initial preconditioning step and followed by pulsed-current deposition with t_{on}:t_{off} = 1 ms:3 ms. A dramatically different result was obtained as no lithium thread was found on the copper surface. Since a slightly improved spatial distribution with an increased number of the lithium islands was seen, the inclusion of the nucleation pulse clearly increased the lithium nuclei density on the copper surface. Nevertheless, lithium islands of various sizes were still observed, and their distribution on the surface was still not homogeneous (see Figure 2d). It is therefore clear that homogeneous 2D lithium nucleation and growth could not be realized in the conventional LP40 electrolyte using this nucleation pulse. There could be two main reasons. First, even with the applied potentiostatic nucleation step it should be difficult to truly achieve a large overpotential at the surface of the copper substrate in the 1.0 M $LiPF_6$ electrolyte since a very high current would be required to decrease the surface concentration of Li^+ sufficiently. Such a high current may give rise to a large iR drop, which means that the true overpotential attained may be too small to allow the generation of nuclei homogeneously on the entire copper surface. It should also be noted that the high current may overload the potentiostat (i.e., the potentiostat cannot supply the high current required between the working and counter electrode to reach the desired working electrode potential). This problem, in fact, limited the stable application of a potentiostatic pulse with a pulse height higher than −0.8 V at the pure copper substrates (see Section S4, Supporting Information). This concentration phenomenon, previously seen for Li|Li symmetric cells, can be attributed to the inherently high redox buffer capacity of a lithium-metal electrode in 1.0 M $LiPF_6$ electrolyte.[40,56] This difficulty in polarizing a Li-metal electrode in 1.0 M $LiPF_6$ electrolyte is, incidentally, the reason why lithium-metal electrodes commonly are used as combined counter and (nonpolarizable) reference electrodes in half-cells, e.g., for electrode material evaluations. It should also be recalled that the potential needed for the electrodeposition of lithium on copper depends on the activity of lithium at the copper surface. As the lithium activity at the surface of the pure copper substrate should be very low, the electrodeposition potential of lithium should, thermodynamically, be higher than 0 V versus Li^+/Li initially. During the electrodeposition process, the potential should then gradually approach 0 V versus Li^+/Li as the activity of lithium at the surface of the copper substrate increases. This phenomenon clearly complicates the electrodeposition of lithium on copper. The second possible reason is that the diffusion of lithium into the copper (which should be particularly evident for small lithium nuclei) may decrease the number of nuclei that actually "survive" on the surface after the nucleation pulse. As it is reasonable to assume that the diffusion of lithium takes place predominantly via the copper grain boundaries, the diffusion may affect the distribution as well as the number of lithium nuclei on the copper surface. This is naturally a problem since the purpose of the nucleation pulse is to generate a multitude of similarly sized lithium nuclei on the surface which then grow during the subsequent deposition step.

One way to address the first issue and hence to facilitate homogeneous nucleation of lithium on the copper surface could be to decrease the Li^+ concentration in the electrolyte, as was previously shown for the lithium nucleation on lithium-metal electrodes.[40] With a lower Li^+ concentration it should be easier to realize a high overpotential since the obtained Li^+ reduction current (and hence the iR drop) should be lower. Analogous lithium electrodeposition experiments, including the use of a nucleation pulse, were therefore carried out in the low-LP40 electrolyte (see Figure 2e,f as well as Figure S1, Supporting Information). Interestingly, similar networks of lithium threads were seen, although much denser than those obtained in the LP40 electrolyte using CC deposition (compare Figure 2e with a). Based on the significantly improved spatial density and distribution of the lithium islands on the copper surface, it is reasonable to conclude that the nucleation process was improved when using the low-LP40 electrolyte (compare Figure 2e,f with c,d). This supports the first hypothesis that a larger overpotential

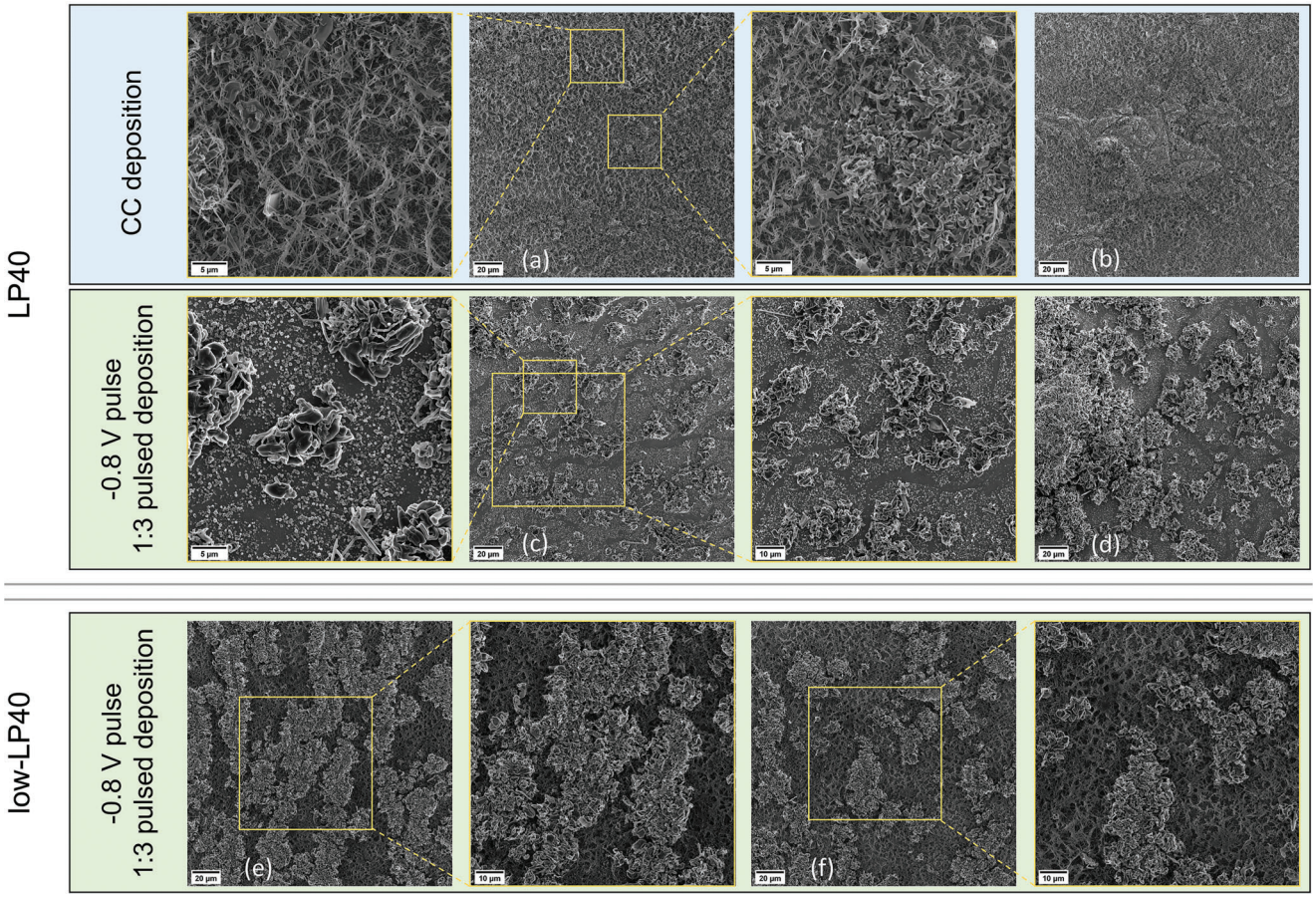

Figure 2. SEM images depicting the morphologies of the lithium electrodeposits obtained on the pure copper substrates in the two electrolytes (i.e., LP40 and low-LP40) using the different deposition protocols (See Figure 1 and the Experimental Section). In (a), (c), (e), and (f), magnifications of the indicated regions are shown, whereas (a) and (b), (c) and (d), and (e) and (f) depict two different regions of the surface.

should be possible to reach during the nucleation pulse when the electrolyte has a lower Li^+ concentration. Nevertheless, homogeneous nucleation on the entire copper surface was still not achieved, which could have been due to the lithium diffusion into the pure copper substrates as explained above.

Since the growth of the lithium (nucleated on the copper surface during the nucleation pulse) was performed using pulsed-current deposition (with t_{on} = 1 ms and t_{off} = 3 ms), it is also interesting to evaluate the influence of the durations of the t_{on} and t_{off} steps on the obtained morphology. By comparing the SEM images presented in Figure 2e,f with those in Figure S1a (Supporting Information) (obtained with t_{on} = 5 ms and t_{off} = 25 ms), it can be seen that the morphologies of the lithium electrodeposits were generally similar using these two different sets of t_{on} and t_{off} in the low-LP40 electrolyte. On the other hand, as shown in Figure S1 (Supporting Information), the pulse height of the potentiostatic nucleation pulse had a significant impact on the lithium electrodeposition, in good agreement with the nucleation theory.

Based on the results presented in Figure 2, it is reasonable to assume that the diffusion of lithium into the copper substrate affects the lithium nucleation on copper. To test this hypothesis, lithium electrodeposition experiments were carried out with prelithiated copper substrates (i.e., copper disks which had been kept in contact with metallic lithium foils at 70 °C under vacuum for 30 d) (see the Experimental Section as well as Section S5, Supporting Information). After this treatment, the average amount of lithium in the prelithiated copper substrates was found to be 11.5 μg cm^{-2} (see Table S1, Supporting Information) using inductively coupled plasma–optical emission spectroscopy (ICP-OES). This value is comparable to that of 10.6 μg cm^{-2} obtained in a previous study in which a piece of copper foil was kept in contact with a metallic lithium foil at 50 °C for one week.[48] After the initial preconditioning step (i.e., open-circuit rest of 30 min followed by the application of a constant current of −0.1 mA cm^{-2} until the cell voltage reached 0 V), the surface of a prelithiated copper substrate was analyzed and compared with that of a pure copper substrate using X-ray photoelectron spectroscopy (XPS). When comparing the XPS results, the surface layers (i.e., SEI layers) formed after the preconditioning step on the two copper substrates were found to be almost identical (see Figure S4 and Section S3, Supporting Information). The major difference between a prelithiated copper substrate and a pure copper substrate was thus the presence of lithium in the former. As can be seen in **Figures 3**, **4**, dramatically improved electrodeposition results were obtained with the prelithiated copper substrates. Using the prelithiated copper substrate and CC deposition in the absence

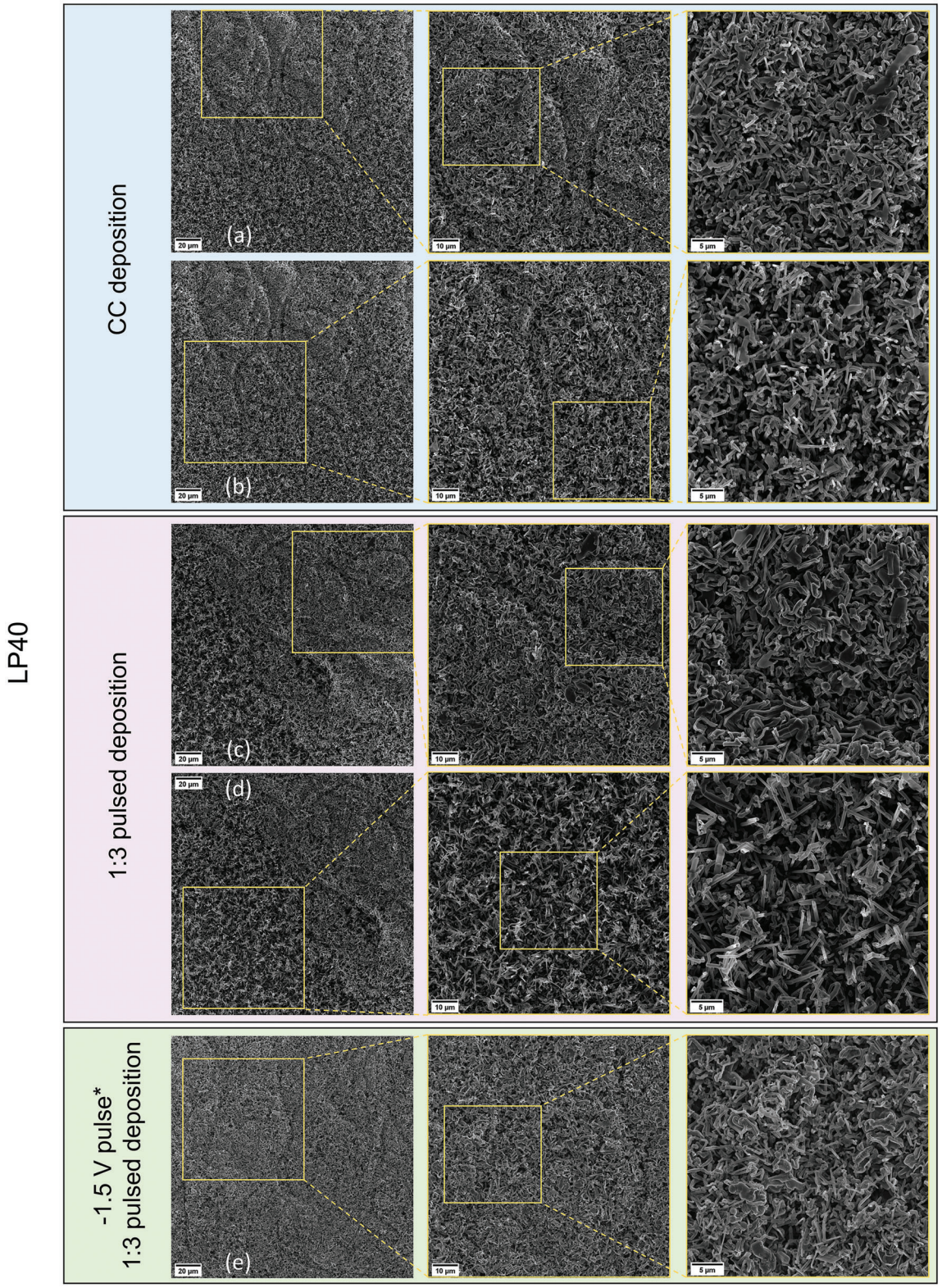

Figure 3. SEM images depicting the morphologies of the lithium electrodeposits obtained on the prelithiated copper substrates in the LP40 electrolyte using the different deposition protocols (See Figure 1 and Materials and Methods). The images in (a) and (b) depict the same region, whereas those in (c) and (d) depict two mostly overlapping regions. In (a–e), magnifications of the indicated regions are also shown. As explained in Section 4 in the Supporting Information, the −1.5 V nucleation pulse could still not be fully implemented in the LP40 electrolyte.

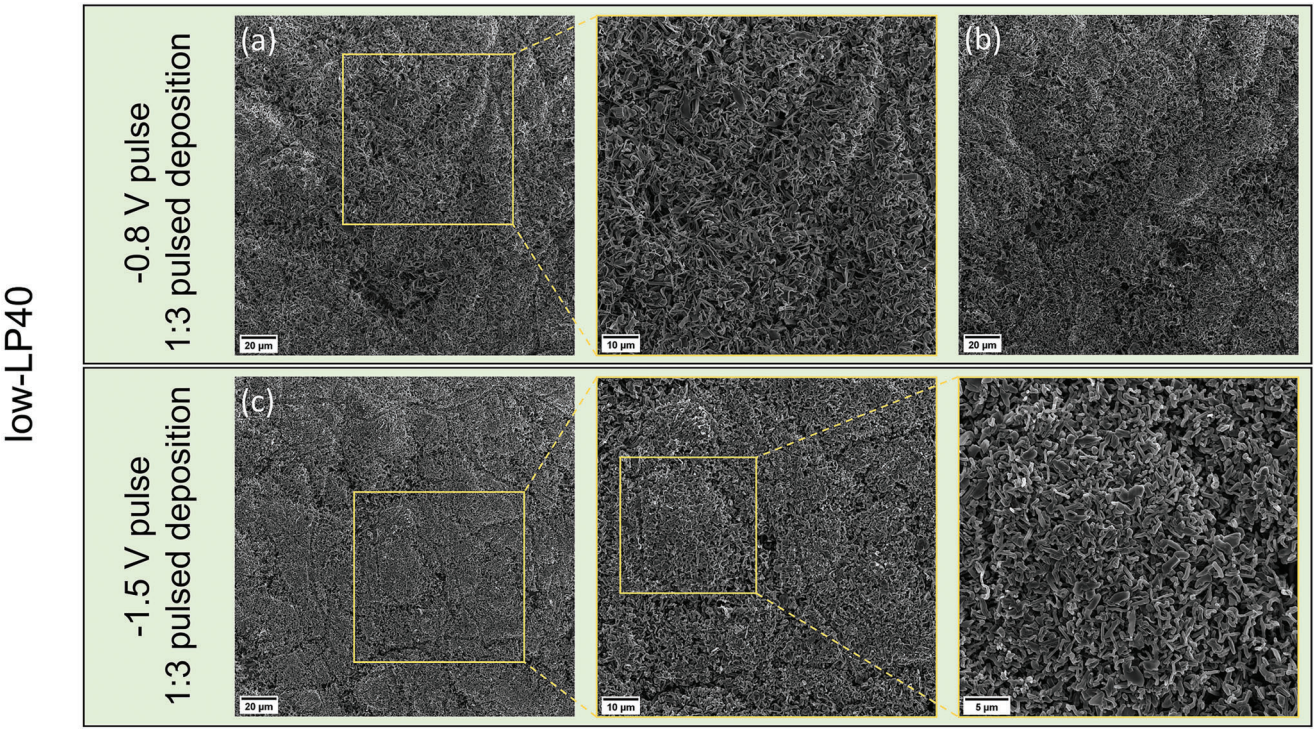

Figure 4. SEM images depicting the morphologies of the lithium electrodeposits obtained on the prelithiated copper substrates in the low-LP40 electrolyte using the pulsed-current deposition protocol with different pulse heights for the preceding potentiostatic nucleation pulse (See Figure 1 and the Experimental Section). In (a) and (c), magnifications of the indicated regions are also shown, whereas (a) and (b) depict two different regions on the surface.

of any nucleation pulse, the lithium electrodeposits obtained in the LP40 electrolyte were more compact and more densely distributed without any formation of loose networks of lithium threads (compare Figure 3a,b with Figure 2a,b). This clearly demonstrates the influence of the lithium diffusion into copper on the lithium nucleation on copper surface, in agreement with the abovementioned hypothesis. It is reasonable to assume that such diffusion was hindered due to lithium-saturated grain boundaries at the surface of the copper. In Figure 3a,b it can, however, still be seen that there were regions with loose lithium "filaments." This inhomogeneous electrodeposition behavior was not significantly improved by using pulsed-current deposition as can be seen in Figure 3c,d. More homogeneous and more compact electrodeposition was, on the other hand, obtained when a potentiostatic nucleation pulse of −1.5 V was included prior to the pulsed-current deposition (see Figure 3e). This illustrates the decisive influence of the initial nucleation on the electrodeposition results. Here, it should be recalled that the pulse height of the potentiostatic nucleation pulse was limited to −0.8 V for the pure copper substrates due to the potentiostat overload issue mentioned above. A potentiostatic nucleation pulse of −1.5 V could, on the other hand, be used with the prelithiated copper substrates. This can be explained by the fact that the lithium activity at the copper surface was increased by the prelithiation, which could have resulted in a decreased lithium deposition current (compared with the lithium deposition on a pure copper substrate) (see Section S4, Supporting Information). Comparing the SEM images in Figure 3e with those in Figure 2c,d, it can be seen that the nucleation pulse was more effective when the copper substrate was prelithiated. These findings hence indicate that both the initial nucleation step and the prelithiation of the copper substrate significantly improved the outcome of the electrodeposition process.

As can be seen in Figure 4 and Figure S2 (Supporting Information), prelithiated copper substrates were also employed in lithium electrodeposition experiments using the low-LP40 electrolyte. The clear difference between the lithium morphologies obtained with a nucleation pulse of −0.8 V on the pure and prelithiated copper substrate (see Figures 2e,f and 4a,b, respectively) indicates that the lithium diffusion into the copper did affect the lithium nucleation conditions. To further test this hypothesis, a corresponding experiment was carried out using a "heated pure copper substrate" (see Figure S3, Supporting Information), which was prepared in the same way as the prelithiated copper substrates but was not subjected to any contact with a lithium foil (see the Experimental Section). The morphology of the lithium electrodeposit obtained on the heated pure copper substrate was found to be more similar to that seen on the pure copper substrate but significantly different from that seen on the prelithiated copper substrate (compare Figure S3, Supporting Information, with Figures 2e,f and 4a,b). This together with the results present in Figure 3 clearly demonstrate that the lithium nucleation (and hence the final electrodeposition result) is affected by the diffusion of lithium into copper and that this issue can be mitigated via chemical prelithiation of the copper substrate. Besides, as the prelithiation step makes the copper substrate more

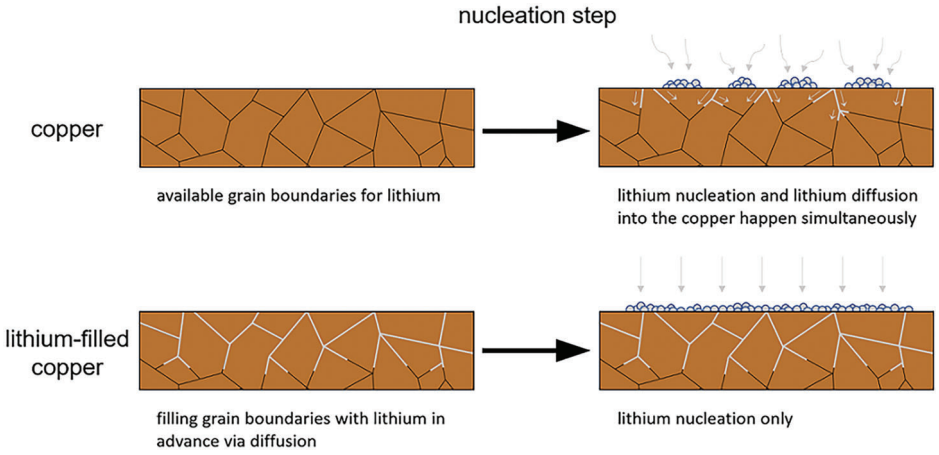

Figure 5. Schematic illustrations of the different lithium nucleation behaviors on copper and prelithiated copper, respectively. Note that a greater number of nuclei, with a more homogeneous distribution, are formed on the prelithiated copper.

similar to a lithium-metal electrode it is also evident that the nucleation on a copper substrate is more complicated than that on a lithium-metal electrode.

The compact and homogeneous lithium electrodeposits seen in Figure 4c, clearly show that the nucleation and then growth of lithium on a prelithiated copper substrate could be further improved by using a nucleation pulse with a pulse height of −1.5 V. This is in good agreement with our nucleation hypothesis as a higher nuclei density (and hence a more homogeneous nucleation on the electrode surface) should be obtained when increasing the overpotential. It should be noted that the increased activity of lithium at the copper surface also facilitated the application of a −1.5 V pulse in the low-LP40 electrolyte (see Section S4, Supporting Information). Moreover, by comparing Figures 4c and 3e, it can also be concluded that the nucleation pulse was more efficient in conjunction with the low-LP40 electrolyte than with the LP40 electrolyte. This can be ascribed to the higher overpotential that should be attained during the nucleation pulse in an electrolyte with a lower Li^+ concentration.

Since pulsed-current deposition was used during the electrodeposition after the nucleation step it is also appropriate to compare the difference between the electrodeposits obtained with the two pulsed-current deposition protocols again. When evaluating the effect of the t_{on} and t_{off} durations used during the pulsed-current deposition of lithium on the prelithiated copper substrate, it was noted that similar and only slightly denser electrodeposits were obtained with t_{on} = 1 ms and t_{off} = 3 ms than with t_{on} = 5 ms and t_{off} = 25 ms (see Figure 4c and Figure S2, Supporting Information). This is in fact in good agreement with the corresponding results for the electrodeposition on pure copper substrates presented in Figure 2e,f and Figure S1a (Supporting Information). This finding together with the results presented in Figure 3a–d clearly indicate that it is the efficiency of the lithium nucleation step that mainly decides the outcome of the electrodeposition. It is consequently unlikely that a poor nucleation step can be compensated for by the use of a subsequent pulsed-current deposition step, in excellent agreement with previous finding for lithium electrodeposition on lithium-metal electrodes.[40]

Based on the experiment results, it can thus be concluded that lithium diffuses into copper substrates and that this affects the lithium nucleation process as schematically illustrated in **Figure 5**. Pure copper foils, especially those prepared by electrodeposition methods (i.e., basically all "battery-grade" copper foils used as current collectors in lithium-based batteries), typically have small grain sizes (down to 0.1 µm or even smaller, see Figure S6a, Supporting Information) and therefore have a lot of grain boundaries.[50,61] These grain boundaries serve as facile lithium diffusion pathways. This further complicates the lithium nucleation process which, in a typical 1.0 M $LiPF_6$ carbonate-based electrolyte, is already intrinsically inhomogeneous and yields the formation of only a few lithium nuclei at certain electrochemically favorable sites. The diffusion of lithium into the copper substrate via the grain boundaries can consequently lead to even fewer lithium nuclei and inhomogeneous nucleation on the copper surface (see Figure 5 top panel). This makes it difficult to obtain the 2D lithium nucleation (and then growth) that is a prerequisite for homogeneous electrodeposition (see Figure 2). Here, it should be noted that theoretical calculations have shown that lithium can enter and diffuse quite swiftly through the crystal structure of copper in the presence of vacancies.[62,63] However, according to the experimental work presented by Lv et al., lithium should be more likely to diffuse through grain boundaries.[49] Further simulation work would clearly be beneficial to provide more insights. According to the nucleation theory, the use of a higher overpotential should lead to a higher number of nuclei with smaller sizes. This should, however, also facilitate the diffusion of lithium into the copper substrate, which could explain the increased lithium uptake previously found when having a higher overpotential.[49] The diffusion of lithium can also explain why the potentiostatic nucleation pulse was ineffective for the pure copper substrates as illustrated in Figure 2. The results, nevertheless, indicate that the influence of the lithium diffusion on the nucleation discussed above can be decreased by chemically prelithiating the copper substrate. This should hinder the lithium diffusion in/into the copper as the grain boundaries become saturated. As a result, a more homogeneous nucleation on the copper surface should be facilitated, especially when using a nucleation pulse. Since the lithium nuclei should be more

stable on the prelithiated copper substrates, 2D lithium nucleation and then growth on the entire copper surface should hence be facilitated (see Figure 5 bottom panel). Moreover, with a prelithiated copper substrate having a higher lithium activity at the surface, nucleation pulses with larger pulse heights can also be used, which further favors the generation of a multitude of similarly sized lithium nuclei on the entire surface. This can in turn give rise to more homogeneous lithium electrodeposition (see Figures 3 and 4).

3. Conclusions

The experimental results clearly demonstrate that the diffusion of lithium into the copper substrate affects the lithium nucleation step. As the latter step sets the scene for the subsequent electrodeposition of lithium, the nucleation step can be said to control the morphology of the lithium electrodeposited on the substrate. During the nucleation step, lithium may diffuse into the copper substrate via the grain boundaries as lithium and copper form a solid solution. As a result, the number of lithium nuclei on the surface decreases and the electrodeposition process becomes less homogeneous. The influence of this effect can, however, be decreased by using chemically prelithiated copper substrates. At the surface of such a copper substrate, the grain boundaries have been filled with lithium, which hinders further diffusion of lithium into the copper during the early stages of the lithium nucleation (and growth). A greater number of lithium nuclei with a more homogeneous distribution are hence obtained on the surface of the prelithiated copper substrate during the nucleation step. The use of prelithiated copper substrates also allows applications of short (i.e., 10 ms long) potentiostatic nucleation pulses with higher pulse heights (e.g., −1.5 V). Such nucleation pulses, especially in combination with a lower Li^+ concentration (e.g., 0.020 rather than 1.0 M) in the electrolyte, facilitate 2D nucleation and growth, in excellent agreement with previous results for lithium electrodeposition on lithium-metal electrodes. The higher nuclei density and thus more compact and homogeneous lithium electrodeposits obtained with such a potentiostatic nucleation pulse stem from the fact that the number of lithium nuclei formed increases when increasing the overpotential applied during the nucleation step. The nucleation pulse approach is, however, less effective when lithium is electrodeposited on a pure copper substrate due to the abovementioned diffusion of lithium into the copper substrate (and also limited pulse heights that can be used).

The potential thermodynamically required for the onset of lithium electrodeposition on copper should vary depending on the activity of lithium at the copper surface. This can readily be seen from the Nernst equation. During the electrodeposition of lithium on a copper substrate, the potential needed for the electrodeposition will therefore become lower and lower as the lithium activity at the surface of the copper substrate gradually increases. This indicates that the electrodeposition of lithium on a copper substrate is more complicated than that on a lithium-metal electrode. Such an effect should also be seen when using any other conductive material as the substrate. When lithium diffuses into the copper substrate, it becomes more and more similar to a lithium-metal electrode. This explains why a nucleation pulse with a larger pulse height (i.e., more negative) can be applied at a prelithiated copper substrate to render a more homogeneous lithium electrodeposition. This finding is in excellent agreement with previous results obtained for lithium nucleation on lithium-metal electrodes.

Since the results show that the use of a pulsed-current (rather than a constant-current) deposition step after the nucleation step only has small influence on the morphologies of the lithium electrodeposits, it is clear that more attention should be paid to an optimization of the nucleation step, e.g., using the approach discussed above. The present results clearly demonstrate the importance of controlling and improving the lithium nucleation process on copper substrates. Based on the discussion of the issues addressed in this study, the understanding of lithium electrodeposition on battery-grade copper foils can be significantly improved. This fundamental research, which focuses on a previously unrecognized effect concerning the electrodeposition of lithium on copper substrates, is very important for the advancement of the underlying science as well as the development of copper-based anode-free lithium-metal batteries.

4. Experimental Section

Materials: The lithium foil (130 µm thick, China Energy Lithium Co., Ltd.), Solupor 3P07A single-layer polyethylene separator (20 µm thick, 83% porosity, Lydall Inc.) and battery-grade copper foil (10 µm thick, Circuit Foil) were obtained from the companies indicated above. The lithium foil was punched into disks with a diameter of 10 mm (i.e., with an area of 0.7854 cm^2). The Solupor 3P07A separators were cut into rectangle pieces of 20 × 40 mm size which then were dried in a Buchi glass oven at 70 °C for 5 h in a glovebox to remove residual moisture prior to the cell assembly. The copper foil was punched into disks with a diameter of 13 mm (i.e., with an area of 1.327 cm^2). The copper disks were then washed by soaking them in glacial acetic acid (ReagentPlus, ≥ 99%, Sigma-Aldrich) for 10 min and dried with argon gas before being quickly transferred into a glovebox.[43,64] The copper disks were then dried in a Buchi glass oven at 30 °C for 2 h and then at 100 °C for 12 h prior to the cell assembly. These copper disks are denoted "pure copper substrates." Two types of electrolytes were used in this study. The first one was LP40 (i.e., 1.0 M $LiPF_6$ in EC:DEC = 1:1 (v/v)), purchased from Solvionic and used as received. The second one, denoted low-LP40, was prepared by diluting the LP40 electrolyte with a solvent mixture of EC (Gotion Inc.): DEC (≥99%, acid < 10 ppm, H_2O < 10 ppm, Sigma-Aldrich) = 1:1 (v/v) and adding tetrabutylammonium hexafluorophosphate ($TBAPF_6$, for electrochemical analysis, ≥99.0%, Sigma-Aldrich) as a supporting salt. Prior to the use, $TBAPF_6$ was dried in a Buchi glass oven at 100 °C for 48 h. The final composition of the low-LP40 electrolyte was 0.020 M $LiPF_6$ and 1.0 M $TBAPF_6$ in EC:DEC = 1:1 (v/v).[40] All preparations were conducted in a glovebox under an argon atmosphere with oxygen and water contents lower than 1 ppm.

Preparation of Prelithiated Copper Substrates: The copper disks (13 mm in diameter) used in the preparation of the prelithiated copper substrates were punched out from the copper foil and transferred into a glovebox without being washed with acetic acid. The copper disks were dried in a Buchi glass oven at 30 °C for 2 h and then at 100 °C for 12 h. The dried copper disks were then brought into contact with a piece of lithium foil, and this assembly was then vacuum sealed into pouches in the glovebox using same type of pouch foils used in the pouch cell assembly (see below). Prior to the sealing, the pouch foils were first dried in a Buchi glass oven at 30 °C for 2 h and then at 70 °C for 12 h. The sealed pouches were left in an oven at 70 °C for 30 d after which the prelithiated copper substrates were retrieved from the pouches. For comparison, some copper disks were

also treated according to the procedure described above, apart from the fact that they were not in contact with any lithium foil (i.e., these copper disks were simply sealed into pouches and kept at 70 °C for 30 d). These reference copper disks are denoted "heated pure copper substrates." All preparations were conducted in a glovebox under an argon atmosphere with oxygen and water contents lower than 1 ppm.

Cell Assembly: The electrochemical deposition experiments were carried out with three-electrode pouch cells in which two lithium disks were used as the counter and reference electrode, respectively, whereas a pure copper substrate, a heated pure copper substrate, or a prelithiated copper substrate was used as the working electrode. It should be noted that it was the lithium-facing side (during the preparation) of the prelithiated copper substrate that was used as the working electrode surface. The reference electrode was separated from the working and counter electrodes using two Solupor separators each soaked with 40 µL electrolyte. Each electrode was connected to a piece of customized copper "tab" that extended out of the cell to serve as an electric terminal. The separators were much larger than the copper working and lithium counter electrodes, so the lithium reference electrode would not block the ion path between the two electrodes that faced each other. As two separators were used the total separator layer thickness was 40 µm with a total amount of electrolyte of 80 µL. An illustration is provided in Figure S8 (Supporting Information). The cell assembly was done in a glovebox under an argon atmosphere with oxygen and water contents lower than 1 ppm.

Electrochemical Deposition Experiments: All electrochemical deposition experiments were conducted using a multichannel potentiostat/galvanostat (VMP-2, Biologic) at room temperature (i.e., 20–25 °C). In all experiments, the cells were subjected to same stack pressure of around 78 kPa. After the cell assembly, cells were first rested for 30 min under open-circuit condition. Prior to the electrodeposition of lithium, the cells were "preconditioned" by applying a current density of −0.1 mA cm^{-2} (i.e., a current of −0.07854 mA) until the cell voltage dropped to 0 V. In the electrodeposition experiments, a 10 ms long potentiostatic nucleation pulse with different pulse heights (i.e., −0.5, −0.8, and −1.5 V) was used. After the nucleation pulse, a 100 ms long pause was applied prior to the pulsed-current deposition to allow the concentration profile generated by the nucleation pulse to relax. The pulsed-current deposition was performed using a current density of −1.0 mA cm^{-2} (i.e., a current of −0.7854 mA) with an on-time (t_{on}) and off-time (t_{off}) of either 1 and 3 ms or 5 and 25 ms long, respectively. The current applied during t_{on} was thus followed by an open-circuit pause during t_{off}. This sequence was repeated until a capacity of −0.5 mAh cm^{-2} was reached (i.e., a current density of −1.0 mA cm^{-2} for a total t_{on} duration of 30 min). For comparison, experiments were also carried out without the nucleation pulse using pulsed-current deposition (−1.0 mA cm^{-2} for −0.5 mAh cm^{-2} with t_{on}:t_{off} = 1 ms:3 ms) and conventional CC deposition (−1.0 mA cm^{-2} for −0.5 mAh cm^{-2}).

Scanning Electron Microscopy: The morphologies of the lithium electrodeposits were studied using high-resolution SEM with a LEO 1550 (Carl Zeiss AG) scanning electron microscope. After an electrodeposition experiment, the pouch cell was transferred back into a glovebox for disassembly. The pure copper substrate, heated pure copper substrate, or prelithiated copper substrate was then retrieved and washed several times with dimethyl carbonate (DMC) (anhydrous, ≥99%, Sigma-Aldrich). The substrate was then dried before being placed on a SEM pin stub. The pin stub was subsequently put into a vial and sealed in a pouch bag in the glovebox before being transported to the microscope. Finally, the pouch bag was opened, and the pin stub was quickly anchored onto the microscope holder and then transferred into the sample chamber within about ten seconds to minimize its exposure to air.

X-Ray Photoelectron Spectroscopy: The XPS measurements were conducted using an AXIS Supra$^+$ spectrometer (Kratos Analytical Ltd.) equipped with monochromatized Al Kα (1486.6 eV) radiation. In the XPS experiments, the surface of the pure copper substrate and prelithiated copper substrate after the initial preconditioning step (i.e., open-circuit rest of 30 min followed by the application of a constant current of −0.1 mA cm^{-2} until the cell voltage reached 0 V) were analyzed. It should be recalled that it was the lithium-facing side (during the preparation) of the prelithiated copper substrate that was used as the working electrode surface and analyzed with XPS. First, the pouch cells were disassembled in an argon-filled glovebox with oxygen and water contents lower than 1 ppm. The copper substrates were rinsed with DMC to remove residual LP40 electrolyte. The substrates were then dried before being mounted on a dedicated sample holder, equipped with an air-tight lid. This was done to make sure that the copper substrates were not exposed to air during their transfer to the load-lock chamber in the XPS system. For each copper sample, a survey measurement was first carried out, followed by scans for the C 1s, O 1s, Li 1s, F 1s, and P 2p regions. The curved fitted C 1s spectra were analyzed using the Igor 9 package software with a linear background. In the analysis, the adventitious carbon peak was set to a binding energy of 284.8 eV as the reference for the charge calibration.[51] The peak assignments of the core-level spectra were based on the results of previous studies (see Section S3, Supporting Information).

Inductively Coupled Plasma–Optical Emission Spectroscopy: ICP-OES measurements were carried out using Avio 500 Scott/Cross-Flow configuration (Perkin Elmer, Inc.) to quantify the lithium amount in the prelithiated copper substrates. The ICP-OES samples were prepared by nitric acid (65%, analytical reagent, VWR) digestion for 48 h. Diluted samples (i.e., ×10 and ×1000 dilution) were prepared by diluting the solutions with milli Q water (ASTM Type I, Fisher Scientific). The calibration with respect to lithium was performed using a solution containing 1 mg L^{-1} of lithium obtained from Multi-element Calibration Standard 3 (Perkin Elmer, Inc.). The lithium peaks for the ×10 and ×1000 sample dilution series were compared with that obtained with the calibration standard solution at a wavelength of 670.784 nm for the quantification.

Supporting Information

Supporting Information is available from the Wiley Online Library or from the author.

Acknowledgements

This work was supported by the Swedish Research Council (VR-2019-04276), The Ångström Advanced Battery Center (ÅABC), and STandUP for Energy. Dr. Yonas Tesfamhret is acknowledged for the assistance during the ICP-OES measurements.

Conflict of Interest

The authors declare no conflict of interest.

Data Availability Statement

The data that support the findings of this study are available from the corresponding author upon reasonable request.

Keywords

anode-free lithium-metal batteries, copper, lithium diffusion, lithium electrodeposition, nucleation

Received: August 10, 2023
Published online: September 3, 2023

[1] R. V. Salvatierra, W. Chen, J. M. Tour, *Adv. Energy Sustainability Res.* **2021**, *2*, 2000110.

[2] S. Nanda, A. Gupta, A. Manthiram, *Adv. Energy Mater.* **2021**, *11*, 2000804.
[3] A. J. Louli, A. Eldesoky, R. Weber, M. Genovese, M. Coon, J. DeGooyer, Z. Deng, R. T. White, J. Lee, T. Rodgers, R. Petibon, S. Hy, S. J. H. Cheng, J. R. Dahn, *Nat. Energy* **2020**, *5*, 693.
[4] Z. Xie, Z. Wu, X. An, X. Yue, J. Wang, A. Abudula, G. Guan, *Energy Storage Mater.* **2020**, *32*, 386.
[5] M. Gao, H. Li, L. Xu, Q. Xue, X. Wang, Y. Bai, C. Wu, *J Energy Chem.* **2021**, *59*, 666.
[6] H. Yuan, X. Ding, T. Liu, J. Nai, Y. Wang, Y. Liu, C. Liu, X. Tao, *Mater. Today* **2022**, *53*, 173.
[7] W. Li, H. Yao, K. Yan, G. Zheng, Z. Liang, Y. M. Chiang, Y. Cui, *Nat. Commun.* **2015**, *6*, 7436.
[8] R. Weber, M. Genovese, A. J. Louli, S. Hames, C. Martin, I. G. Hill, J. R. Dahn, *Nat. Energy* **2019**, *4*, 683.
[9] S. Jurng, Z. L. Brown, J. Kim, B. L. Lucht, *Energy Environ. Sci.* **2018**, *11*, 2600.
[10] J. Qian, B. D. Adams, J. Zheng, W. Xu, W. A. Henderson, J. Wang, M. E. Bowden, S. Xu, J. Hu, J. G. Zhang, *Adv. Funct. Mater.* **2016**, *26*, 7094.
[11] J. Qian, W. A. Henderson, W. Xu, P. Bhattacharya, M. Engelhard, O. Borodin, J. G. Zhang, *Nat. Commun.* **2015**, *6*, 6362.
[12] D. W. Kang, J. Moon, H. Y. Choi, H. C. Shin, B. G. Kim, *J. Power Sources* **2021**, *490*, 229504.
[13] C. Yan, Y.-X. Yao, X. Chen, X.-B. Cheng, X.-Q. Zhang, J.-Q. Huang, Q. Zhang, *Angew. Chem.* **2018**, *130*, 14251.
[14] D. Liu, X. Xiong, Q. Liang, X. Wu, H. Fu, *Chem. Commun.* **2021**, *57*, 9232.
[15] S. Liu, X. Ji, N. Piao, J. Chen, N. Eidson, J. Xu, P. Wang, L. Chen, J. Zhang, T. Deng, S. Hou, T. Jin, H. Wan, J. Li, J. Tu, C. Wang, *Angew. Chem., Int. Ed.* **2021**, *60*, 3661.
[16] H. Zhao, D. Lei, Y. B. He, Y. Yuan, Q. Yun, B. Ni, W. Lv, B. Li, Q. H. Yang, F. Kang, J. Lu, *Adv. Energy Mater.* **2018**, *8*, 1800266.
[17] X. Ma, Z. Liu, H. Chen, *Nano Energy* **2019**, *59*, 500.
[18] Y. Gu, H. Y. Xu, X. G. Zhang, W. W. Wang, J. W. He, S. Tang, J. W. Yan, D. Y. Wu, M. Sen Zheng, Q. F. Dong, B. W. Mao, *Angew. Chem., Int. Ed.* **2019**, *58*, 3092.
[19] N. Zhang, S. H. Yu, H. D. Abruña, *Nano Res.* **2020**, *13*, 45.
[20] A. A. Assegie, C. C. Chung, M. C. Tsai, W. N. Su, C. W. Chen, B. J. Hwang, *Nanoscale* **2019**, *11*, 2710.
[21] P. Zhai, Y. Wei, J. Xiao, W. Liu, J. Zuo, X. Gu, W. Yang, S. Cui, B. Li, S. Yang, Y. Gong, *Adv. Energy Mater.* **2020**, *10*, 1903339.
[22] R. Zhang, X. R. Chen, X. Chen, X. B. Cheng, X. Q. Zhang, C. Yan, Q. Zhang, *Angew. Chem., Int. Ed.* **2017**, *56*, 7764.
[23] K. Yan, Z. Lu, H. Lee, F. Xiong, P. Hsu, Y. Li, J. Zhao, S. Chu, Y. Cui, *Nat. Energy* **2016**, *1*, 16010.
[24] V. Pande, V. Viswanathan, *ACS Energy Lett.* **2019**, *4*, 2952.
[25] N. Xu, L. Li, Y. He, Y. Lu, L. Li, Y. Lu, Y. Tong, *J. Mater. Chem. A* **2020**, *8*, 6229.
[26] J. Qian, S. Wang, Y. Li, M. Zhang, F. Wang, Y. Zhao, Q. Sun, L. Li, F. Wu, R. Chen, *Adv. Funct. Mater.* **2021**, *31*, 2006950.
[27] N. Zhang, S. H. Yu, H. D. Abruña, *Chem. Commun.* **2019**, *55*, 10124.
[28] R. Greff, R. Peat, L. M. Peter, D. Pletcher, J. Robinson, *Instrumental Methods in Electrochemistry*, Ellis Horwood, Hemel Hempsted, UK **1990**.
[29] M. Paunovic, M. Schlesinger, *Fundamentals of Electrochemical Deposition*, Wiley, New York **1998**.
[30] J. Mostany, B. R. Scharifker, K. Saavedra, C. Borrás, *Russ. J. Electrochem.* **2008**, *44*, 652.
[31] K. Yan, J. Wang, S. Zhao, D. Zhou, B. Sun, Y. Cui, G. Wang, *Angew. Chem., Int. Ed.* **2019**, *58*, 11364.
[32] J. Wang, W. Huang, A. Pei, Y. Li, F. Shi, X. Yu, Y. Cui, *Nat. Energy* **2019**, *4*, 664.
[33] Y. Han, Y. Jie, F. Huang, Y. Chen, Z. Lei, G. Zhang, X. Ren, L. Qin, R. Cao, S. Jiao, *Adv. Funct. Mater.* **2019**, *29*, 1904629.
[34] M. Genovese, A. J. Louli, R. Weber, C. Martin, T. Taskovic, J. R. Dahn, *J. Electrochem. Soc.* **2019**, *166*, A3342.
[35] A. Pei, G. Zheng, F. Shi, Y. Li, Y. Cui, *Nano Lett.* **2017**, *17*, 1132.
[36] W. Chang, J. H. Park, N. S. Dutta, C. B. Arnold, D. A. Steingart, *Chem. Mater.* **2020**, *32*, 2803.
[37] J. Xiao, Q. Li, Y. Bi, M. Cai, B. Dunn, T. Glossmann, J. Liu, T. Osaka, R. Sugiura, B. Wu, J. Yang, J. G. Zhang, M. S. Whittingham, *Nat. Energy* **2020**, *5*, 561.
[38] B. Thirumalraj, T. T. Hagos, C. J. Huang, M. A. Teshager, J. H. Cheng, W. N. Su, B. J. Hwang, *J. Am. Chem. Soc.* **2019**, *141*, 18612.
[39] S. Wang, X. Yin, D. Liu, Y. Liu, X. Qin, W. Wang, R. Zhao, X. Zeng, B. Li, *J. Mater. Chem. A* **2020**, *8*, 18348.
[40] D. Rehnlund, C. Ihrfors, J. Maibach, L. Nyholm, *Mater. Today* **2018**, *21*, 1010.
[41] S. Xiong, L. Nyholm, A. Matic, C. Zhang, *Mater. Today Energy* **2022**, *28*, 101060.
[42] W. Huang, D. T. Boyle, Y. Li, Y. Li, A. Pei, H. Chen, Y. Cui, *ACS Nano* **2019**, *13*, 737.
[43] A. B. Gunnarsdóttir, C. V. Amanchukwu, S. Menkin, C. P. Grey, *J. Am. Chem. Soc.* **2020**, *142*, 20814.
[44] D. Rehnlund, J. Pettersson, K. Edström, L. Nyholm, *ChemistrySelect* **2018**, *3*, 2311.
[45] S. Menkin, C. A. Okeefe, A. B. Gunnarsdóttir, S. Dey, F. M. Pesci, Z. Shen, A. Aguadero, C. P. Grey, *J. Phys. Chem. C* **2021**, *125*, 16719.
[46] P. G. Kitz, M. J. Lacey, P. Novák, E. J. Berg, *Anal. Chem.* **2019**, *91*, 2296.
[47] J. Shu, M. Shui, F. Huang, D. Xu, Y. Ren, L. Hou, J. Cui, J. Xu, *Electrochim. Acta* **2011**, *56*, 3006.
[48] D. Rehnlund, F. Lindgren, S. Böhme, T. Nordh, Y. Zou, J. Pettersson, U. Bexell, M. Boman, K. Edström, L. Nyholm, *Energy Environ. Sci.* **2017**, *10*, 1350.
[49] S. Lv, T. Verhallen, A. Vasileiadis, F. Ooms, Y. Xu, Z. Li, Z. Li, M. Wagemaker, *Nat. Commun.* **2018**, *9*, 2152.
[50] R. Rupp, B. Caerts, A. Vantomme, J. Fransaer, A. Vlad, *J. Phys. Chem. Lett.* **2019**, *10*, 5206.
[51] F. Linsenmann, M. Trunk, P. Rapp, L. Werner, R. Gernhäuser, R. Gilles, B. Märkisch, Z. Révay, H. A. Gasteiger, *J. Electrochem. Soc.* **2020**, *167*, 100554.
[52] D. Rehnlund, Z. Wang, L. Nyholm, *Adv. Mater.* **2022**, 2108827.
[53] H. Okamoto, *J. Phase Equilib. Diffus.* **2011**, *32*, 172.
[54] A. Vlad, A. L. M. Reddy, A. Ajayan, N. Singh, J. F. Gohy, S. Melinte, P. M. Ajayan, *Proc. Natl. Acad. Sci. USA* **2012**, *109*, 15168.
[55] Y. Liu, M. Sun, Y. Yuan, Q. Wu, H. Wang, Y. He, Z. Lin, F. Zhou, M. Ling, C. Qian, C. Liang, J. Lu, *Adv. Funct. Mater.* **2020**, *30*, 1910249.
[56] Y. K. Huang, R. Pan, D. Rehnlund, Z. Wang, L. Nyholm, *Adv. Energy Mater.* **2021**, *11*, 2003674.
[57] M. S. Chandrasekar, M. Pushpavanam, *Electrochim. Acta* **2008**, *53*, 3313.
[58] Q. Li, S. Tan, L. Li, Y. Lu, Y. He, *Sci. Adv.* **2017**, *3*, e1701246.
[59] M. Z. Mayers, J. W. Kaminski, T. F. Miller, *J. Phys. Chem. C* **2012**, *116*, 26214.
[60] B. D. Adams, J. Zheng, X. Ren, W. Xu, J. G. Zhang, *Adv. Energy Mater.* **2018**, *8*, 1702097.
[61] M. Kim, H. S. Park, *Appl. Microsc.* **2022**, *52*, 2.
[62] Z. Xiong, S. Shi, C. Ouyang, M. Lei, L. Hu, Y. Ji, Z. Wang, L. Chen, *Phys. Lett. A* **2005**, *337*, 247.
[63] Y. Zhuang, Z. Zou, B. Lu, Y. Li, D. Wang, M. Avdeev, S. Shi, *Chin. Phys. B* **2020**, *29*, 068202.
[64] K. L. Chavez, D. W. Hess, *J. Electrochem. Soc.* **2001**, *148*, G640.